Applied Catalysis B: Environmental 180 (2016) 726–732

Contents lists available at ScienceDirect

Applied Catalysis B: Environmental

journal homepage: www.elsevier.com/locate/apcatb

Can environmental pharmaceuticals be photocatalytically degraded and completely mineralized in water using g-C_3N_4/TiO_2 under visible light irradiation?—Implications of persistent toxic intermediates

Guiying Li [a], Xin Nie [a,b], Yanpeng Gao [a], Taicheng An [a,*]

[a] State Key Laboratory of Organic Geochemistry and Guangdong Key Laboratory of Environmental Protection and Resources Utilization, Guangzhou Institute of Geochemistry, Chinese Academy of Sciences, Guangzhou 510640, China
[b] University of Chinese Academy of Sciences, Beijing 100049, China

ARTICLE INFO

Article history:
Received 31 May 2015
Received in revised form 8 July 2015
Accepted 10 July 2015
Available online 22 July 2015

Keywords:
g-C_3N_4/TiO_2
Antiviral pharmaceutical
Photocatalysis
Visible light
Risk assessment

ABSTRACT

This study investigated the feasibility of photocatalytic degradation and detoxification of antiviral pharmaceuticals using a novel graphitic carbon nitride (g-C_3N_4)/TiO_2 hybrid photocatalyst under visible light irradiation. The results indicated that acyclovir is difficult to be mineralized, although it could be completely degraded within 90 min using this high stable hybrid photocatalyst. Further investigation found that three main intermediates (P1, P2, and P3) produced during the photocatalytic process remain persistent, due to the low oxidation potential of the highest occupied molecular orbital (HOMO) of g-C_3N_4. The acute and chronic toxicities of acyclovir and these three intermediates were assessed at three trophic levels with theoretical calculated data obtained by the "ecological structure-activity relationships" program. The results found that toxicities of two of the intermediates P1 and P2 were lower than the toxicity of acyclovir to three levels tested organisms. However, the aquatic toxicity of the third intermediate P3, guanine, was more than double that of acyclovir, although most toxicity values still fell in the same toxic class except for the chronic impact on daphnia (acyclovir is harmful, and the guanine intermediary is toxic). This study's findings support the selection of new photocatalysts for purifying and detoxifying environmental pharmaceuticals in water.

1. Introduction

Pharmaceuticals can significantly improve worldwide public health and quality of life when used to treat infectious diseases. However, the overuse of pharmaceuticals, especially antibiotics, threatens both the environment and human health. Pharmaceuticals and their metabolites are becoming increasing ubiquitous in aquatic environments and even in drinking water. These chemicals are introduced as a result of human and animal use, or as residues from manufacturers and hospitals [1–3]. The continuous usage and perfusion of these pharmaceutical compounds in water environments may make them "pseudo-persistent," even if they have short half-lives [4,5]. Further, most pharmaceuticals, including antibiotics, may pose serious threats to the ecosystem and human health, even at low concentrations [6–9].

Effectively removing pharmaceuticals from water is a challenge [10–12]. Conventional wastewater and drinking water purification treatments do not always efficiently eliminate pharmaceuticals, because they were never designed to remove these emerging organic contaminants (EOCs). Furthermore, conventional biological treatment processes create an environmentally suitable hotpot for antibiotic resistant bacteria and genes, because bacteria are continuously mixed with antibiotics at sub-inhibitory concentrations [13,14]. Therefore, new technologies are needed to effectively eliminate these pharmaceuticals from water.

Semiconductor TiO_2 photocatalysis has emerged as a promising technology to purify wastewater containing a wide array of organics, including pharmaceuticals [12,15–17]. Its benefits include superior photocatalytic oxidation ability, nontoxic and stable characteristics. However, TiO_2 photocatalysis uses UV light with λ less than 380 nm because of its wide band gap. This hampers its potential practical applications in environmental remediation, where visible light is used [18].

Recently, graphitic carbon nitride (g-C_3N_4) has attracted worldwide attention because of its low band gap, which can lead to the efficient light harvesting within the visible light region. This unique property and its electric conductivity make it promising for potential applications and theoretical predictions [19–21]. Wang

* Corresponding author. Fax: +86 20 85290706.
E-mail address: antc99@gig.ac.cn (T. An).

http://dx.doi.org/10.1016/j.apcatb.2015.07.014
0926-3373/

et al. first used g-C_3N_4 as a photocatalyst to successfully produce hydrogen [21], and since then, research has explored H_2 evolution and organics degradation [22,23]. However, pure g-C_3N_4 has some shortcomings, such as rapid recombination of photo-generated electron–hole pairs, resulting in low photocatalytic activity [24,25]. Therefore, different g-C_3N_4-based photocatalysts have been synthesized to promote the visible light photocatalytic activity of g-C_3N_4.

Among these abundant g-C_3N_4—based photocatalysts, g-C_3N_4/TiO_2 has been frequently constructed because of its enhancement of electron hole separations and subsequent high photocatalytic activity [26,27]. Nevertheless, most of these works had mainly focused on using g-C_3N_4/TiO_2 composite as a catalyst under visible light irradiation to produce H_2 [28,29] or to degrade common organics, such as dye [30–32], phenol [33,34], formaldehyde [35], or dibenzothiphene [36]. To date, there has been little research into the photocatalytic decontamination ability of g-C_3N_4/TiO_2 and its mineralization mechanism for EOCs in water, especially for the decomposition of pharmaceuticals. We have, however, successfully used this newly-prepared promising photocatalyst to explore the photocatalytic inactivation and further decomposition of gram-negative bacterium *Escherichia coli* [37].

In this study, this fabricated hybrid photocatalyst was tested for its possible use to decontaminate environmental pharmaceuticals in water, given the coexistence of pharmaceuticals and biohazards in wastewater and drinking water. First, the photocatalytic degradation and mineralization of acyclovir (an antiviral drug) in the aquatic environment were attempted using this visible-light-driven g-C_3N_4/TiO_2 composite as photocatalyst. Second, the decomposition mechanism was studied in detail, to identify various degradation intermediates. Third, the potential risks posed by acyclovir and its photocatalytic degradation intermediates were also evaluated using a high throughput computational tool, the "ecological structure-activity relationships" (ECOSAR) program.

2. Experimental section

2.1. Synthesis of hybrid photocatalysts

The g-C_3N_4/TiO_2 hybrid photocatalyst with visible light response was synthesized using a facile hydrothermal-calcination approach [37]. In this process, 1.0 g NH_4F (analytical grade, Guangzhou Chemical Reagent Factory, China) and 1.0 g melamine (analytical grade, Guangzhou Chemical Reagent Factory, China) were first dispersed into 40 mL deionized water, and then exposed to ultrasound for 30 min. The mixtures were transferred into 100 mL Teflon-line autoclaves with the cleaned Ti foils (99.6% purity, 50 × 25 × 0.16 mm, Baoji Haiji Titanium & Nickel Co., Ltd., China) placed vertically; the material was then hydrothermally treated at 150 °C for 72 h in an oven. After the hydrothermal reaction, the resultant materials were collected using a centrifuge, thoroughly washed with distilled water, and dried at 80 °C. Materials were then heated to 550 °C in alumina crucibles sealed with aluminum foil in a muffle furnace for 4 h, at a heating rate of 20 °C min^{-1}. As a control for comparison, the pure TiO_2 was prepared without added melamine and with 1.0 g NH_4F at a hydrothermal temperature of 150 °C for 72 h. The pure g-C_3N_4 was also synthesized by directly heating melamine; the TiO_2 was prepared using identical heating procedure for the control.

2.2. Procedure for photocatalytic degradation

The photocatalytic degradation of acyclovir (98.0% purity, Tokyo Chemical Industry Co., Ltd, Japan) was conducted in a 110 mL glass reactor. Thirty milligrams of the catalyst was first added to a 100 mL acyclovir solution (10 ppm). The reaction solution was kept at approximately 25 °C and stirred with a magnetic stirrer throughout the experiment. Dark adsorption was allowed for 30 min to establish an adsorption-desorption equilibrium; then, a 300 W Xe lamp (λ>420 nm with an UV filter, light intensity: 30 mW cm^{-2}) was activated. Next, 3 mL sample solutions were collected at different time intervals; each was filtered through a 0.22 μm Millipore filter for later analysis.

Acyclovir concentrations were determined using high pressure liquid chromatography (HPLC, Agilent 1200) with a dual absorbance detector (DAD) detector at a wavelength of 252 nm equipped with a Kromasil ODS (5 μm, 4.6 mm × 250 mm) reverse-phase column. The mobile phase was a mixture of methanol and water (V:V = 1:9) with a flow rate of 1.0 mL min^{-1}. HPLC tandem mass spectrometry (HPLC/MS/MS, Waters Xevo TQ, Micromass MS Technologies, UK) was used to identify degradation intermediates.

2.3. Total organic carbon (TOC)

The total organic carbon (TOC) in the degradation solution at different intervals was measured using a TOC analyzer (Shimadzu TOC–VCPH, Kyoto).

2.4. Eco-toxicity assessment

The acute and chronic toxicities of acyclovir and its degradation intermediates were assessed using calculated data from the ECOSAR program [38]. This program has successfully predicted aquatic toxicities and has been used to screen environmental EOCs [39,40]. Exposure risks to aquatic organisms were considered at three different trophic levels: green algae, daphnia, and fish. Acute toxicity is expressed using EC_{50} values (the pollutant concentration that inhibits green algae growth by 50% growth after 96 h) and LC_{50} values (the pollutant concentration that leads to the death of 50% fish and daphnia after 96 and 48 h exposures, respectively). The lowest values for each LC_{50} and EC_{50} endpoint were used to yield the most conservative estimates.

3. Results and discussion

3.1. The photocatalytic degradation of acyclovir under visible light irradiation

This study examined the photocatalytic degradation of a typical antivirus pharmaceutical, acyclovir, to evaluate the visible light activity of hybrid photocatalysts comprised of g-C_3N_4 and TiO_2, prepared at various conditions. Pure g-C_3N_4 and TiO_2 were used as control photocatalysts to provide a baseline comparison. As Fig. 1a shows, the acyclovir was stable with pure TiO_2 under visible light irradiation; only a very slight change of acyclovir concentration was seen within 300 min (5 h).

Comparatively, the photocatalytic degradation of acyclovir using pure g-C_3N_4 was much more efficient than with TiO_2 under visible light irradiation. Complete acyclovir degradation was achieved within 240 min using g-C_3N_4/TiO_2 as photocatalyst. The degradation rate constant was 0.0076 min^{-1} (Table S1). This is because g-C_3N_4 has a small band-gap, and thus can harvest photons within the visible light region to generate e^- and h^+ pairs [41,42]. In addition to the h^+ of g-C_3N_4, the generated e^- can subsequently produce other reactive species (RSs), such as $^{\bullet}O_2^-$ and H_2O_2. These species can also attack and decompose acyclovir.

The g-C_3N_4/TiO_2 hybrid photocatalyst prepared at 1.0 g NH_4F at a hydrothermal temperature of 150 °C for 72 h demonstrated the highest rate constant for acyclovir degradation, at 0.0157 min^{-1}. This was approximately twice as fast as the pure g-C_3N_4 and the complete degradation of acyclovir could be achieved only within

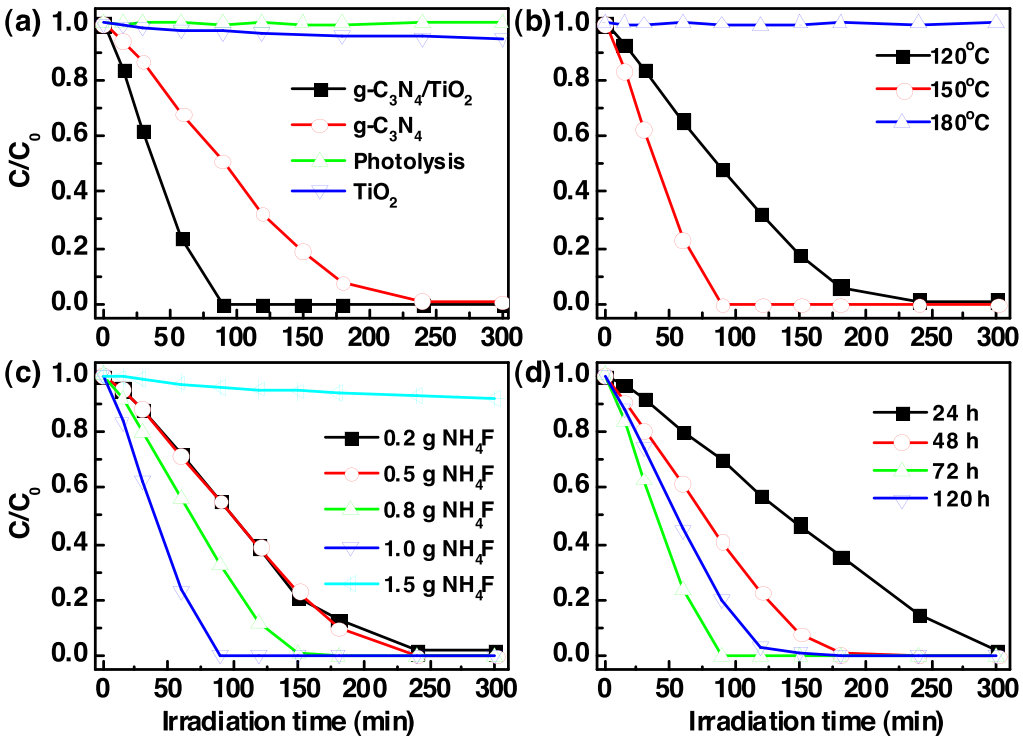

Fig. 1. The photocatalytic degradation of acyclovir under visible light irradiation using (a) pure TiO_2, g-C_3N_4, and g-C_3N_4/TiO_2; (b) the photocatalysts prepared at 1.0 g NH_4F and treated for 72 h with different hydrothermal temperatures; (c) the photocatalysts prepared at hydrothermal temperature of 150 °C treated for 72 h with different NH_4F concentrations; (d) the photocatalysts prepared at 1.0 g NH_4F and hydrothermal temperature of 150 °C treated with different times.

90 min. Higher photocatalytic activity of g-C_3N_4/TiO_2 occurred because of the existed large number of amino, carboxyl, and hydroxyl groups in the hybrid photocatalyst; these could form cross-linked connections and covalent bonds between g-C_3N_4 and TiO_2 [37]. This could strengthen the chemical interaction and may be of significance to the transfer carriers, inducing a synergetic effect to enhance visible light absorbance and photocatalytic activity [43–45].

For the samples prepared at different hydrothermal temperatures (Fig. 1b), the highest rate constant (0.0157 min^{-1}) for the photocatalytic degradation of acyclovir was obtained using the sample fabricated at 150 °C (Table S1). Lower and higher hydrothermal temperatures decrease the photocatalytic activity of the resultant catalysts. For example, the rate constant of the catalyst obtained at 120 °C (0.0081 min^{-1}) was low and only slightly higher than that of the pure g-C_3N_4. In addition, the sample prepared at 180 °C also had very low photocatalytic activity under visible light irradiation. This is due to that only solid agglomerated g-C_3N_4 and flower-like anatase TiO_2 were obtained at hydrothermal temperatures of 120 °C and 180 °C, respectively. In contrast, the photocatalyst prepared at the hydrothermal temperature of 150 °C is composed of micron-sized TiO_2 spheres wrapped with lamellar g-C_3N_4, significantly improving the visible light absorption of the catalyst and effectively separating photo-generated electron-hole pairs [37].

This study also assessed the photocatalytic degradation of acyclovir using the photocatalysts prepared with different added amount of NH_4F (Fig. 1c). When less than 0.5 g NH_4F was added, the rate constants of the obtained catalysts were slightly less than that of pure g-C_3N_4 (Table S1); complete removal of acyclovir could be achieved within 240 min. Increasing NH_4F from 0.8 to 1.0 g, significantly increased degradation rate constants from 0.0097 to 0.0157 min^{-1}, and complete degradation of acyclovir could be achieved within 150 and 90 min, respectively. This suggests that photocatalytic activity was enhanced with more NH_4F. However, further increasing NH_4F to 1.5 g led to a dramatic decrease of the photocatalytic activity of resultant catalyst, with a rate constant of 0.0005 min^{-1}, and the removal of only 8% acyclovir within 300 min. This drop is because the low amount of additional NH_4F could not efficiently etch the Ti foil to produce good TiO_2 crystal seeds in the solution. As such, only g-C_3N_4 was seen in the prepared samples [37]. Too much NH_4F (e.g. 1.5 g) would led to the formation of the highly acidic compound NH_4HF_2 in hot water. This would result in complete melamine hydrolysis, generating tricyanicacid rather than g-C_3N_4 [46]. That is, only micron-sized TiO_2 spheres with the diameter of *ca.* 4 μm were observed under these conditions [37].

Hydrothermal time also significantly affected the photocatalytic activity of the resultant catalysts (Fig. 1d). Setting hydrothermal time to less than 72 h increased photocatalytic activities of the samples, and acyclovir could be completely degraded within 90 min. The rate constants for the photocatalysts prepared at 24, 48, and 72 h were obtained as 0.0041, 0.0099, and 0.0157 min^{-1}, respectively (Table S1). Further increasing hydrothermal time to 120 h decreased photocatalytic activity of the prepared photocatalysts, and decreased the rate constant to 0.0135 min^{-1} for the photocatalytic degradation of acyclovir. The reason is that the prepared sample is composed of micron-sized TiO_2 spheres and wrapped with lamellar g-C_3N_4. According to the X-ray diffraction (XRD) characterization, anatase TiO_2 and g-C_3N_4 diffraction peak intensities increase rapidly as hydrothermal time increased from 24 to 72 h, then dropped slightly as the hydrothermal time extended to 120 h [37].

All these results suggest that the hydrothermal temperature and treatment time, as well as the added amount of NH_4F, significantly affect the visible light photocatalytic activity of acyclovir degradation. The optimal conditions for the g-C_3N_4/TiO_2 hybrid photocatalyst for the degradation of acyclovir were: 1.0 g NH_4F, at a hydrothermal temperature of 150 °C, for 72 h. The optimal g-C_3N_4/TiO_2 hybrid photocatalyst consists of micron-sized TiO_2 spheres (average diameter: *ca.* 2 μm), wrapped with lamel-

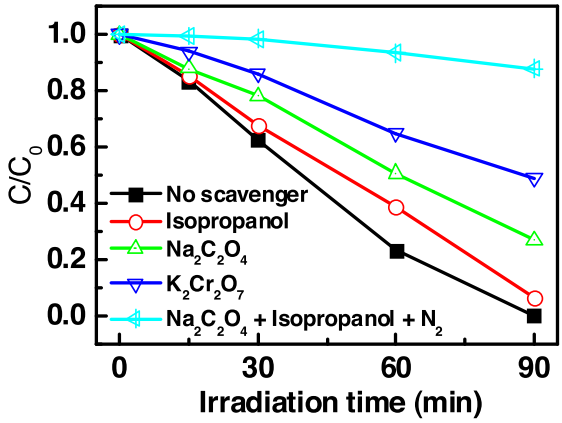

Fig. 2. Photocatalytic degradation of acyclovir with different scavengers by g-C_3N_4/TiO_2 hybrid photocatalyst prepared with 1.0 g NH_4F and hydrothermal temperatures of 150 °C for 72 h.

lar g-C_3N_4 (thickness: *ca.* 2 nm), with narrowing band-gap (*ca.* 2.48 eV). The highest photocatalytic degradation efficiency of acyclovir (100% within 90 min) was seen with the highest rate constant of 0.0157 min^{-1}.

Similar results were seen in our previous work, which found that the best photocatalytic inactivation efficiency of *E. coli* occurred at these same conditions [37]. Furthermore, the stability of the resultant optimal g-C_3N_4/TiO_2 hybrid photocatalyst was also evaluated. As Fig. S1 shows, after 5 recycling runs, there was a negligible decrease in acyclovir degradation efficiency using the optimal hybrid photocatalyst. This suggests that g-C_3N_4/TiO_2 has high stability and great potential practical applications for environmental purification under visible light irradiation.

3.2. Contribution of different RSs.

During the photocatalytic treatment process, different reactive species (RSs), such as h^+, •OH, e^-, H_2O_2, and $O_2^{\bullet-}$, may be generated and attack the acyclovir using g-C_3N_4/TiO_2 as a photocatalyst. As such, experiments were done to add individual scavengers to remove the respective RSs in the degradation reaction and to further identify their contributions to the photocatalytic degradation of acyclovir. Studied scavengers included $Na_2C_2O_4$ (10 mM) for h^+, $K_2Cr_2O_7$ (50 μM) for e^-, and isopropanol (10 mM) for •OH [47,48]. As Fig. 2 and Table S2 show, without adding any scavengers, faster degradation of acyclovir was observed, with a photocatalytic degradation rate constant of 0.0157 min^{-1}. However, adding $Na_2C_2O_4$ significantly inhibited acyclovir degradation, with an acyclovir degradation rate constant of only 0.0083 min^{-1}.

This result indicates that the valence band (VB) h^+ played an important role in the photocatalytic degradation of acyclovir in this system. Nevertheless, when •OH was scavenged by isopropanol, the photocatalytic degradation efficiency dropped only slightly, compared to when no scavengers were used. This further confirmed that it is VB h^+, rather than its derivatives •OH, that play an important role in this photocatalytic degradation system.

To further discriminate the role of the conduction band (CB) RSs, $K_2Cr_2O_7$ was added to quench e^-. Photocatalytic degradation efficiencies, as well as the rate constant (0.0073 min^{-1}), decreased even more than those when $Na_2C_2O_4$ was added, indicating that CB e^- also played an important role in this system. To further determine whether the acyclovir was attacked by e^- itself or its derivatives $O_2^{\bullet-}$ or H_2O_2, a solution was added containing isopropanol and $Na_2C_2O_4$ degassed with N_2. This was done to reserve only CB e^-. Only a slight decrease in the acyclovir concentration was observed, suggesting that CB e^- only plays a minor role in this photocatalytic process [47]. As such, other RSs derived from CB e^-, such as $O_2^{\bullet-}$ and H_2O_2, were the predominant contributors to acyclovir degradation when g-C_3N_4/TiO_2 was used as the photocatalyst. Therefore, the photo-generated h^+ and $O_2^{\bullet-}$ or H_2O_2 derived from CB e^- were the main RSs for the photocatalytic degradation of acyclovir. These RSs directly oxidized and decomposed acyclovir, while •OH only played a minor role in this visible light driven system [49,50].

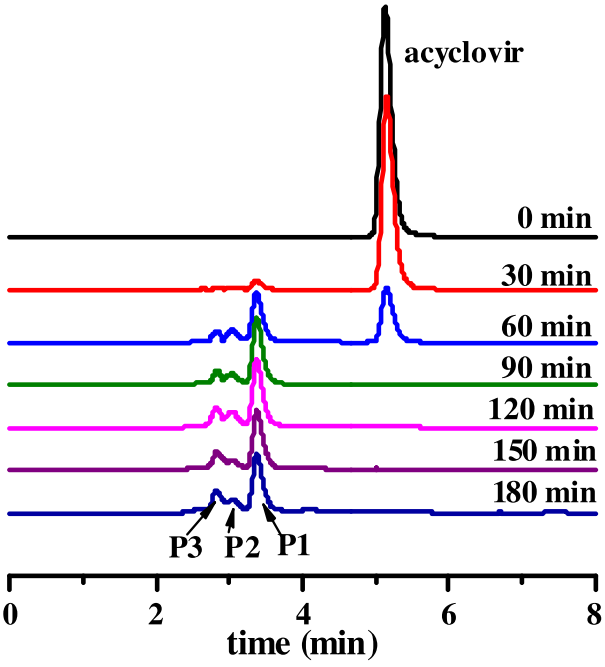

Fig. 3. The HPLC chromatograms obtained for the photocatalytic treated acyclovir samples at different reaction intervals by g-C_3N_4/TiO_2 hybrid photocatalyst under visible light irradiation. Retention time: t_R(acyclovir) = 5.1 min; t_R(P1) = 3.4 min; t_R(P2) = 3.0 min; t_R(P3) = 2.8 min.

The finding that h^+ and $O_2^{\bullet-}$ act as the main RSs in the photocatalytic degradation of organics generally aligns with other research that has used g-C_3N_4-based photocatalysts [51,52]; however, •OH was found to be dominantly responsible for acyclovir degradation in the UV/TiO_2 system in our previous work [12]. These different results imply that the presence of g-C_3N_4 with a TiO_2 photocatalyst can significantly affect the physic-chemical properties of hybrid photocatalysts and influence main RSs in the photocatalytic organic treatment process. This may lead to different degradation mechanisms.

3.3. Photocatalytic degradation mechanism of acyclovir

The photocatalytic degradation intermediates of acyclovir by this visible-light-driven photocatalyst were also detected and identified with a HPLC/MS/MS. Fig. 3 shows the HPLC chromatograms of acyclovir degradation at different irradiation times. For untreated samples, there was an absorption peak with a retention time (t_R) of 5.1 min. This points to the original acyclovir molecule. After 30 min of treatment, the acyclovir concentration decreased approximately 20%.

Simultaneously, three degradation intermediates (P1 with t_R 3.4 min, P2 with t_R 3.0 min and P3 with t_R 2.8 min) were detected. All of them were more hydrophilic than the original compound acyclovir, although these peaks are very tiny. After 60 min of treatment, the acyclovir peak significantly decreased, while the three degradation intermediates increased. The intermediate P1 increased the most. After 90 min of treatment, the acyclovir peak decreased to below the detection limit; the intermediate P1 concentration

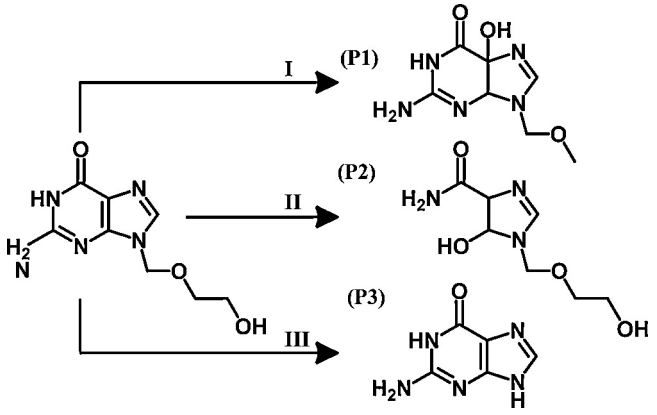

Fig. 4. Proposed visible-light-driven photocatalytic degradation pathway of acyclovir in water by g-C_3N_4/TiO_2 hybrid photocatalyst.

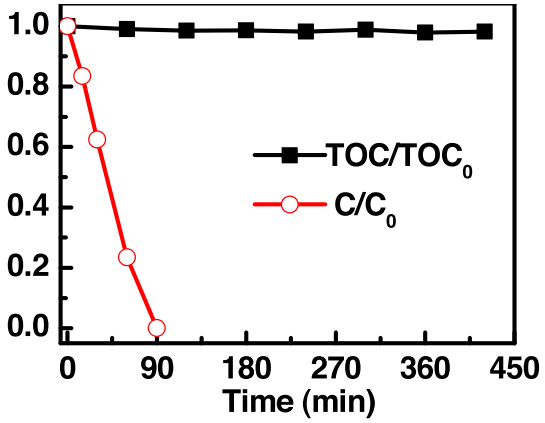

Fig. 5. TOC reduction during the photocatalytic treatment of acyclovir.

increased gradually, and the peaks of intermediates P2 and P3 did not significantly change. As the reaction time continued, the three intermediate peak heights are quite stable.

These trends can also be seen in the UV absorption spectrum during the acyclovir decomposition process (Fig. S2). Acyclovir structures and fragmentation patterns, as well as those of its degradation intermediates, were all identified from MS data and are illustrated in Figs. S3 and S4, respectively. The main intermediate, P1 with *m/z* 214, was first obtained during the photocatalytic degradation process. This corresponds with the monohydroxylation of the purine ring and the breakdown of CC bond from the side chain. The intermediate P2 with *m/z* 205 resulted from the breakdown of the acyclovir purine ring. By prolonging the irradiation time, another intermediate, P3 with *m/z* 152, was identified as guanine; this was produced through the loss of the side chain (Fig. 4). All three intermediates were also detected during the photocatalytic degradation of acyclovir in the previously studied UV/TiO_2 system [12]. To confirm the accurate identification of the intermediate, the identity of intermediate P3 (guanine), was also validated using the fragmentation pattern of an authentic standard.

This research also investigated the extent of mineralization of acyclovir during the photocatalytic degradation process, using the visible-light-driven hybrid g-C_3N_4/TiO_2 photocatalyst (Fig. 5). Unexpectedly, the TOC concentration of the degradation solution showed negligible change, even after 7 h of irradiation time, while the acyclovir could be degraded completely within 90 min. This suggests that the degradation intermediates were very persistent, and could not be fully mineralized by the RSs produced in this system under visible light irradiation. This trend was also seen during the acyclovir biodegradation process [53], although TOC removal can be decreased to more than 60% (within 120 min) in the UV/TiO_2 system [12]. This outcome also differs from the conclusion that the photocatalytic inactivation of bacteria, *E. coli*, could be completely achieved by this fabricated g-C_3N_4/TiO_2 hybrid photocatalyst under visible light irradiation [37].

It was worth investigating why the degradation intermediates of acyclovir are so persistent and difficult to be mineralized during the photocatalytic process. One reason may be the low capacity of the g-C_3N_4/TiO_2 hybrid photocatalyst. That is, under visible light irradiation, the g-C_3N_4 is photoexcited, separating e^- and h^+ in the lowest (LUMO) and highest occupied molecular orbital (HOMO), respectively. The CB of TiO_2 with -0.4 V oxidation potential is more positive than the LUMO of g-C_3N_4 (−1.12 V); the VB of TiO_2 (+2.8 V) is lower than the HOMO of g-C_3N_4 (+1.57 V) [54,55]. As such, the e^-

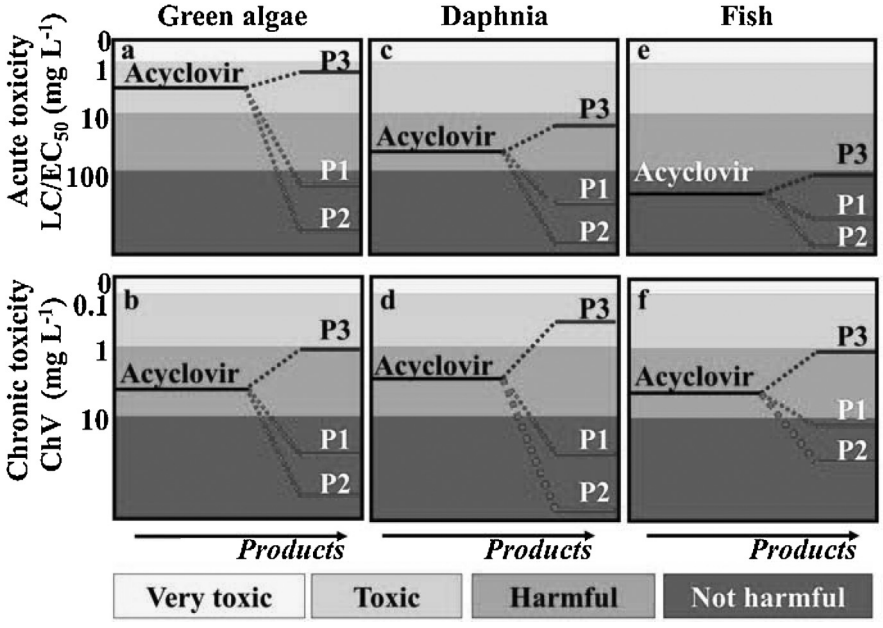

Fig. 6. Theoretical calculated data of aquatic toxicity of acyclovir as zwell as its degradation intermediates.

could efficiently transfer from the LUMO of photoexcited g-C_3N_4 to the CB of TiO_2.

As a result, a large number of e^- could accumulate onto the TiO_2 surface, forming $O_2^{\bullet-}$ and then H_2O_2 through the scavenging of e^- by the adsorbed O_2 on the catalyst surface. Although the suitably matching CB and VB levels effectively promote charge separations and suppress photo-generated e^- and h^+ pair recombination [56], the oxidation potential of the HOMO of g-C_3N_4 was only 1.57 V. For this reason, this system cannot completely mineralize acyclovir and its degradation intermediates, due to the low oxidation potential of the RS produced and not directly oxidized to generate •OH (2.7 V). Despite this, the bacteria can be successfully inactivated and further decomposed under certain conditions [37].

3.4. Toxicity predictions of degradation intermediates formed during the photocatalytic degradation of acyclovir

The ECOSAR program was used to predict the acute and chronic toxicities of acyclovir and its degradation intermediates at three trophic levels. As Fig. 6 shows, the acute toxicity of acyclovir was estimated as LC_{50} for fish and daphnia, and as EC_{50} for green algae. These values were 1.76×10^3, 69.2, and 2.62 mg L^{-1}, respectively. According to the European Union criteria (Table S3), acyclovir is classified as not harmful for fish, harmful for daphnia, and toxic for green algae. Chronic toxicity values (ChVs) of acyclovir were predicted as 3.89 mg L^{-1} for fish, 2.04 mg L^{-1} for daphnia, and 3.62 mg L^{-1} for green algae. Based on the Chinese hazard evaluation guidelines for new chemical substances (HJ/T 154–2004) (Table S3), acyclovir is classified as chronically harmful at all three trophic levels.

To better understand the toxicity evolution during the photocatalytic degradation of acyclovir, the acute and chronic eco-toxicities of the three persistent intermediates were also calculated. As Fig. 6 shows, both for acute and chronic toxicities, the LC_{50} (or EC_{50}) and ChV values of the intermediates P1 and P2 increased greatly, and were about 3 (Fish ChV) to 454 times (Green algae EC_{50}) higher than those of acyclovir. The value was classified as non-harmful level for all three tested organisms.

The degradation route I to form the P1 intermediate (the monohydroxylation of purine ring and the breakdown of CC bond from the side chain of acyclovir) and the degradation route II to form the P2 intermediate (the breakdown of purine ring in acyclovir) were very effective in detoxifying acyclovir. The resulting intermediates P1 and P2 were less toxic than acyclovir during this photocatalytic degradation process. However, for degradation route III, the P3 (guanine) (formed from the losing the side chain from acyclovir) was more toxic than acyclovir. That is, the LC_{50} (or EC_{50}) and ChV values of acyclovir were more than twice those of intermediate P3, although most of these values fell in the same class except daphnia ChV (acyclovir is harmful and intermediate P3 is toxic). These calculated eco-toxicities aligned with our previous experiments found that guanine (P3) was a main intermediate and that the toxicity to *Daphnia magna* increased gradually and then decreased when extending the reaction time in the UV/TiO_2 system [12]. The toxicity did not decrease because of the lower oxidation potential of the HOMO of g-C_3N_4.

4. Conclusion

In summary, typical pharmaceuticals like acyclovir can be efficiently photocatalytically degraded using a g-C_3N_4/TiO_2 hybrid photocatalyst under visible light irradiation. However, this process produces three persistent intermediates. Unfortunately, intermediary ecotoxicity, particularly the chronic toxicity of guanine (P3) to daphnia, was significantly enhanced during the photocatalytic degradation process. Given that the process produces persistent intermediaries that resist mineralization, caution is needed. Using g-C_3N_4/TiO_2 as a visible light driven photocatalyst to decompose pharmaceuticals must be carefully considered before applying the technique to detoxify real pharmaceutical pollutants.

Acknowledgments

This is contribution No. IS–2097 from GIGCAS. This work was supported by National Natural Science Funds for Distinguished Young Scholars (41425015), National Nature Science Foundation of China (21077104 and 41373103) and Earmarked Fund of SKLOG (SKLOG2011A02).

Appendix A. Supplementary data

Supplementary data associated with this article can be found, in the online version, at http://dx.doi.org/10.1016/j.apcatb.2015.07.014

References

[1] K.S. Le Corre, C. Ort, D. Kateley, B. Allen, B.I. Escher, J. Keller, Environ. Int. 45 (2012) 99–111.
[2] H.W. Leung, L. Jin, S. Wei, M.M.P. Tsui, B.S. Zhou, L.P. Jiao, P.C. Cheung, Y.K. Chun, M.B. Murphy, P.K.S. Lam, Environ. Health Perspect. 121 (2013) 839–846.
[3] T. Azuma, N. Nakada, N. Yamashita, H. Tanaka, Environ. Sci. Technol. 46 (2012) 12873–12881.
[4] T.C. An, H. Yang, G.Y. Li, W.H. Song, W.J. Cooper, X.P. Nie, Appl. Catal. B: Environ. 94 (2010) 288–294.
[5] T.C. An, H. Yang, W.H. Song, G.Y. Li, H.Y. Luo, W.J. Cooper, J. Phys. Chem. A 114 (2010) 2569–2575.
[6] G.M. Bruce, R.C. Pleus, S.A. Snyder, Environ. Sci. Technol. 44 (2010) 5619–5626.
[7] R.S. Prosser, P.K. Sibley, Environ. Int. 75 (2015) 223–233.
[8] C. Larson, Science 347 (2015) 704.
[9] A.B.A. Boxall, M.A. Rudd, B.W. Brooks, D.J. Caldwell, K. Choi, S. Hickmann, E. Innes, K. Ostapyk, J.P. Staveley, T. Verslycke, G.T. Ankley, K.F. Beazley, S.E. Belanger, J.P. Berninger, P. Carriquiriborde, A. Coors, P.C. DeLeo, S.D. Dyer, J.F. Ericson, F. Gagne, J.P. Giesy, T. Gouin, L. Hallstrom, M.V. Karlsson, D.G.J. Larsson, J.M. Lazorchak, F. Mastrocco, A. McLaughlin, M.E. McMaster, R.D. Meyerhoff, R. Moore, J.L. Parrott, J.R. Snape, R. Murray-Smith, M.R. Servos, P.K. Sibley, J.O. Straub, N.D. Szabo, E. Topp, G.R. Tetreault, V.L. Trudeau, G. Van Der Kraak, Environ. Health Perspect. 120 (2012) 1221–1229.
[10] T.C. An, J.B. An, H. Yang, G.Y. Li, H.X. Feng, X.P. Nie, J. Hazard. Mater. 197 (2011) 229–236.
[11] H. Yang, T.C. An, G.Y. Li, W.H. Song, W.J. Cooper, H.Y. Luo, X.D. Guo, J. Hazard. Mater. 179 (2010) 834–839.
[12] T.C. An, J.B. An, Y.P. Gao, G.Y. Li, H.S. Fang, W.H. Song, Appl. Catal. B-Environ. 164 (2015) 279–287.
[13] L. Rizzo, C. Manaia, C. Merlin, T. Schwartz, C. Dagot, M.C. Ploy, I. Michael, D. Fatta-Kassinos, Sci. Total Environ. 447 (2013) 345–360.
[14] B.K. Biswal, A. Mazza, L. Masson, R. Gehr, D. Frigon, Water Res. 50 (2014) 245–253.
[15] J.B. An, G.Y. Li, T.C. An, W.H. Song, H.X. Feng, Y.J. Lu, Catal. Today (2015), http://dx.doi.org/10.1016/j.cattod.2015.1001.1004
[16] J. Choi, H. Lee, Y. Choi, S. Kim, S. Lee, S. Lee, W. Choi, J. Lee, Appl. Catal. B-Environ. 147 (2014) 8–16.
[17] S. Ramasundaram, H.N. Yoo, K.G. Song, J. Lee, K.J. Choi, S.W. Hong, J. Hazard. Mater. 258 (2013) 124–132.
[18] Z.Y. Wang, Y.Y. Liu, B.B. Huang, Y. Dai, Z.Z. Lou, G. Wang, X.Y. Zhang, X.Y. Qin, Phys. Chem. Chem. Phys. 16 (2014) 2758–2774.
[19] L. Ge, F. Zuo, J.K. Liu, Q. Ma, C. Wang, D.Z. Sun, L. Bartels, P.Y. Feng, J. Phys. Chem. C 116 (2012) 13708–13714.
[20] Y.J. Zhang, T. Mori, J.H. Ye, M. Antonietti, J. Am. Chem. Soc. 132 (2010) 6294–6295.
[21] X.C. Wang, K. Maeda, A. Thomas, K. Takanabe, G. Xin, J.M. Carlsson, K. Domen, M. Antonietti, Nat. Mater. 8 (2009) 76–80.
[22] G.P. Dong, Y.H. Zhang, Q.W. Pan, J.R. Qiu, J. Photoch. Photobio. C 20 (2014) 33–50.
[23] Y.J. Zhang, T. Mori, J.H. Ye, Sci. Adv. Mater. 4 (2012) 282–291.
[24] Z.W. Zhao, Y.J. Sun, F. Dong, Nanoscale 7 (2015) 15–37.
[25] H.Q. Sun, G.L. Zhou, Y.X. Wang, A. Suvorova, S.B. Wang, ACS Appl. Mater. Inter. 6 (2014) 16745–16754.
[26] J.W. Zhou, M. Zhang, Y.F. Zhu, Phys. Chem. Chem. Phys. 17 (2015) 3647–3652.
[27] J.C. Shen, H. Yang, Q.H. Shen, Y. Feng, Q.F. Cai, Crystengcomm 16 (2014) 1868–1872.
[28] Y.P. Zang, L.P. Li, Y.S. Xu, Y. Zuo, G.S. Li, J. Mater. Chem. A 2 (2014) 15774–15780.

[29] J.X. Wang, J. Huang, H.L. Xie, A.L. Qu, Int. J. Hydrogen. Energ. 39 (2014) 6354–6363.
[30] K. Sridharan, E. Jang, T.J. Park, Appl. Catal. B-Environ. 142 (2013) 718–728.
[31] N. Boonprakob, N. Wetchakun, S. Phanichphant, D. Waxler, P. Sherrell, A. Nattestad, J. Chen, B. Inceesungvorn, J. Colloid Interface Sci. 417 (2014) 402–409.
[32] L. Zhang, D.W. Jing, X.L. She, H.W. Liu, D.J. Yang, Y. Lu, J. Li, Z.F. Zheng, L.J. Guo, J. Mater. Chem. A 2 (2014) 2071–2078.
[33] S.S. Zhao, S. Chen, H.T. Yu, X. Quan, Sep. Purif. Technol. 99 (2012) 50–54.
[34] C. Miranda, H. Mansilla, J. Yanez, S. Obregon, G. Colon, J. Photoch. Photobio. A 253 (2013) 16–21.
[35] J.G. Yu, S.H. Wang, J.X. Low, W. Xiao, Phys. Chem. Chem. Phys. 15 (2013) 16883–16890.
[36] C. Wang, W.S. Zhu, Y.H. Xu, H. Xu, M. Zhang, Y.H. Chao, S. Yin, H.M. Li, J.G. Wang, Ceram. Int. 40 (2014) 11627–11635.
[37] G.Y. Li, X. Nie, J.Y. Chen, T.C. An, P.K. Wong, H.M. Zhang, H.J. Zhao, H. Yamashita, Water Res. (2015), http://dx.doi.org/10.1016/j.watres.2015.05.053
[38] ECOSAR, http://www.epa.gov/oppt/newchems/tools/21ecosar.htm, 2014.
[39] O.A.H. Jones, N. Voulvoulis, J.N. Lester, Water Res. 36 (2002) 5013–5022.
[40] Y.P. Gao, Y.M. Ji, G.Y. Li, T.C. An, Water Res. 49 (2014) 360–370.
[41] Y.J. Cui, J.S. Zhang, G.G. Zhang, J.H. Huang, P. Liu, M. Antonietti, X.C. Wang, J. Mater. Chem. 21 (2011) 13032–13039.
[42] Y.G. Li, J.A. Zhang, Q.S. Wang, Y.X. Jin, D.H. Huang, Q.L. Cui, G.T. Zou, J. Phys. Chem. B 114 (2010) 9429–9434.
[43] S.C. Yan, S.B. Lv, Z.S. Li, Z.G. Zou, Dalton. Trans. 39 (2010) 1488–1491.
[44] D. Mitoraj, H. Kisch, Angew. Chem. Int. Edit. 47 (2008) 9975–9978.
[45] J.S. Zhang, G.G. Zhang, X.F. Chen, S. Lin, L. Mohlmann, G. Dolega, G. Lipner, M. Antonietti, S. Blechert, X.C. Wang, Angew. Chem. Int. Edit. 51 (2012) 3183–3187.
[46] J.G. Yu, Q.J. Xiang, J.R. Ran, S. Mann, Crystengcomm 12 (2010) 872–879.
[47] H.S. Fang, Y.P. Gao, G.Y. Li, J.B. An, P.K. Wong, H.Y. Fu, S.D. Yao, X.P. Nie, T.C. An, Environ. Sci. Technol. 47 (2013) 2704–2712.
[48] W.J. Wang, Y. Yu, T.C. An, G.Y. Li, H.Y. Yip, J.C. Yu, P.K. Wong, Environ. Sci. Technol. 46 (2012) 4599–4606.
[49] S.C. Yan, Z.S. Li, Z.G. Zou, Langmuir 26 (2010) 3894–3901.
[50] S.X. Ge, L.Z. Zhang, Environ. Sci. Technol. 45 (2011) 3027–3033.
[51] F.T. Li, Y. Zhao, Q. Wang, X.J. Wang, Y.J. Hao, R.H. Liu, D.S. Zhao, J. Hazard. Mater. 283 (2015) 371–381.
[52] C. Chang, Y. Fu, M. Hu, C.Y. Wang, G.Q. Shan, L.Y. Zhu, Appl. Catal. B-Environ. 142 (2013) 553–560.
[53] C. Prasse, M. Wagner, R. Schulz, T.A. Ternes, Environ. Sci. Technol. 45 (2011) 2761–2769.
[54] X.S. Zhou, F. Peng, H.J. Wang, H. Yu, Y.P. Fang, Chem. Commun. 47 (2011) 10323–10325.
[55] J.X. Sun, Y.P. Yuan, L.G. Qiu, X. Jiang, A.J. Xie, Y.H. Shen, J.F. Zhu, Dalton. Trans. 41 (2012) 6756–6763.
[56] Y. Wang, X.C. Wang, M. Antonietti, Angew. Chem. Int. Edit. 51 (2012) 68–89.